Modulation of a Salt Link Does Not Affect Binding of Phosphate to Its Specific Active Transport Receptor[†,‡]

Nanhua Yao,[§] Polly S. Ledvina,[||] Abha Choudhary,[||] and Florante A. Quiocho*[,§,||]

Department of Biochemistry and Howard Hughes Medical Institute, Baylor College of Medicine, Houston, Texas 77030

Received November 9, 1995; Revised Manuscript Received December 11, 1995[⊗]

ABSTRACT: Electrostatic interactions are among the key forces determining the structure and function of proteins. These are exemplified in the liganded form of the receptor, a phosphate binding protein from *Escherichia coli*. The phosphate, completely dehydrated and buried in the receptor, is bound by 12 hydrogen bonds as well as a salt link with Arg 135. We have modulated the ionic attraction while preserving the hydrogen bonds by mutating Asp 137, also salt linked to Arg 135, to Asn, Gly, or Thr. High-resolution crystallographic analysis revealed that Gly and Thr (but not Asn) mutant proteins have incorporated a more electronegative Cl^- in place of the Asp carboxylate. That no dramatic effect on phosphate affinity was produced by these ionic perturbations indicates a major role for hydrogen bonds and other local dipoles in the binding and charge stabilization of ionic ligands.

The interaction between a protein and its ligand forms the basis of biological selectivity and activity. The selectivity of active transport of phosphate into a cell is an excellent example of regulation achieved through exceedingly high protein receptor−ligand specificity. The role of electrostatic interactions in this specificity is the subject of this paper.

The highly specific complex between the phosphate-binding protein (PBP)[1] and phosphate (Luecke & Quiocho, 1990), stabilized entirely by electrostatic interactions (including van der Waals forces), provides an excellent system in which to examine the role of electrostatics in ligand recognition and affinity. PBP is a member of a family of about 50 proteins which serve as initial high-affinity receptors for permeases or active transport of a wide variety of ligands in bacterial cells [reviewed in Lam and Saier (1993)]. The permease for phosphate is distinct from that for sulfate, which requires a sulfate-binding protein (SBP) (Medvecsky & Rosenberg, 1971; Pardee et al., 1966), and at physiological pH, PBP and SBP exhibit no overlap in specificity. This exquisite specificity prevents one nutrient from becoming an inhibitor of transport for the other. Understanding the structural and biochemical basis for the specificity and electrostatic interactions of PBP, as well as SBP, has been one major focus of investigations in our laboratory.

Fully consistent with the stringent specificity of the PBP receptor, the phosphate, which is completely dehydrated and sequestered deep in the cleft between the two domains, forms 12 hydrogen bonds (11 with donor groups and 1 with the acceptor group) as well as one salt link with the guanidinium group of Arg 135 (Figure 1) (Luecke & Quiocho, 1990). The presence of the negatively charged Asp 56, the hydrogen bond acceptor, is unusual for an anion-binding site, but this residue is essential for two key roles in conferring exquisite specificity. It recognizes the phosphate by way of its donatable proton (Figure 1) and inhibits, by charge repulsion, the binding of the sulfate dianion at physiological pH. Evidently, even with a potential 11 hydrogen bonds with the donor groups and one salt link, the PBP receptor is unable to bind sulfate.

In the PBP−phosphate complex, we have found a unique opportunity to probe the contribution of an ionic interaction without interfering with the hydrogen-bonding geometry. Not all of the positive charge from the guanidinium of Arg 135 is neutralized by the salt link with the phosphate, because the guanidinium further shares similar ionic and bidentate hydrogen-bonding interactions with the carboxylate of Asp 137 (Figure 1). Since there is no isosteric neutral side chain to replace a guanidinium group involved in intricate interactions, our best approach is to modulate the Coulombic interaction with the phosphate while preserving the role of Arg 135 as a donor of hydrogen bonds to the phosphate. This paper described this approach, combining site-directed mutagenesis, ligand-binding measurement, and high-resolution crystallographic analysis.

MATERIALS AND METHODS

Site-Directed Mutagenesis, Protein Purification, and Phosphate-Binding Assay. Oligonucleotide-directed mutagenesis (Kunkel et al., 1987), PBP gene expression, and protein purification were conducted as previously described (Wang et al., 1994). The codon GAT (Asp) at position 137 in the wild-type PBP was replaced with AAT (Asn), GGT (Gly), or ACT (Thr) to form the respective mutant proteins. Mutants were identified by dideoxy DNA sequencing using a Sequenase kit from U.S. Biochemical Corp. Upon subcloning into the expression vector, mutations were further verified by dideoxy sequencing of the double-strand DNA. Mutant derivatives of PBP were purified, and phosphate-binding activity (K_d) was determined following procedures used previously (Wang et al., 1994).

[†] Supported by an NIH grant (R01GM21371).

[‡] Five coordinate sets have been deposited in the Protein Data Bank (ID codes 2ABH, 1QUI, 1QUJ, 1QUK, and 1QUL).

* To whom correspondence may be addressed at HHMI, BCM, Houston, TX 77030.

[§] Department of Biochemistry.

[||] Howard Hughes Medical Institute.

[⊗] Abstract published in *Advance ACS Abstracts,* February 1, 1996.

[1] Abbreviations: PBP, phosphate-binding protein; SBP, sulfate-binding protein; rms, root mean square.

0006-2960/96/0435-2079$12.00/0

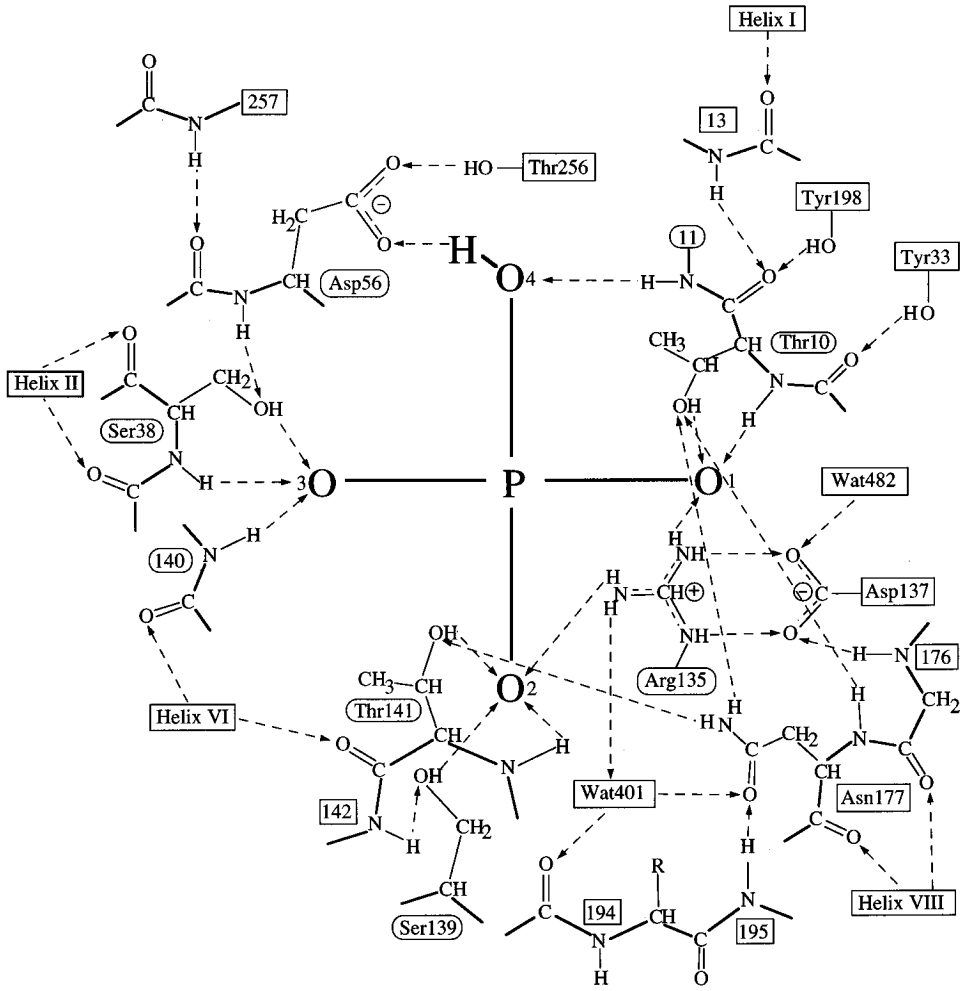

FIGURE 1: Schematic diagram of the hydrogen-bonding and ionic interactions between PBP and phosphate and additional networks of hydrogen bonds [adapted from Luecke and Quiocho (1990)]. Residues making direct hydrogen bonds to the phosphate are outlined by ellipses, and those making further hydrogen bond networks (or second shell) are enclosed in rectangles. If only the peptide backbone groups are involved, the residues are not identified. PBP binds phosphate at high pH and low pH where the dibasic and monobasic forms, respectively, exist almost exclusively (see Table 2; Wang et al., 1994). The mechanism for monobasic phosphate recognition is less clear than that depicted in the figure for dibasic phosphate (Luecke & Quiocho, 1990).

Table 1: Structure Refinement Statistics

parameter	native	137N	137G(Cl)	137G(Br)	137T(Cl)
R-factor	0.177	0.180	0.190	0.190	0.187
R-free	0.190	0.189	0.209	0.218	0.205
resolution range (Å)	8.0−1.7	8.0−1.7	8.0−1.9	8.0−1.9	8.0−1.7
unique reflections/% completeness	36051/97	31740/85	25510/96	24857/93	30383/82
rms deviation from ideal bond distances (Å)	0.013	0.013	0.015	0.015	0.016
rms deviation from ideal bond angle (deg)	1.61	1.62	1.78	1.79	1.72
average B-factor (Å^2)					
all atoms	19.3	13.1	17.3	16.2	8.7
polyglycine backbone	15.8	9.7	14.4	13.5	6.5
side chain	18.1	11.6	16.3	15.2	9.1

Structure Determination. Mutant derivatives of PBP were crystallized as previously described (Luecke & Quiocho, 1990; Wang et al., 1994). The crystals were harvested in a stabilizing solution of 20% poly(ethylene glycol) 6000, 2 mM potassium phosphate, 50 mM potassium chloride, and 20 mM potassium acetate, pH 4.5. The space group ($P2_12_12_1$) and unit cell dimensions of the various mutant crystals are virtually identical to those of the wild-type crystals (Luecke & Quiocho, 1990). Diffraction data were collected on an ADSC dual area detector system (Wang et al., 1994). The *R*-merge values for the four protein mutant diffraction data sets shown in Table 1 range from 0.047 to 0.072. No σ cutoffs were applied on the data used in the refinement except for 137T(Cl), where 2σ was applied. The X-PLOR program Version 3.1 (Brünger, 1992), with the parameters of Engh and Huber (1991), was used in the structure refinement. The CHAIN program (Sack, 1988) was used in fitting the model to the electron density maps and examination of the structures. The mutant structures were determined by direct phasing with the full set of coordinates of the 1.7 Å native structure (re-refined using X-PLOR, Table 1) minus only the Asp 137 side chain. After the refinement was initiated with one cycle of rigid body refinement, the *R*-factor dropped to about 0.22, confirming the very high degree of isomorphism between the wild-type and the four mutant structures. This was followed by several rounds of

Table 2: Dissociation Constants for Phosphate Binding to Wild-Type and Mutant PBPs[a]

Asp 137 mutation	K_d (μM) pH 4.5	K_d (μM) pH 8.5
Native	2.72 (0.82)	0.31 (0.03)
Asn	3.29 (0.53)	0.26 (0.03)
Gly(Cl)	1.80 (0.36)	0.19 (0.01)
Thr(Cl)	6.50 (1.13)	0.72 (0.11)

[a] Phosphate-binding activities of the wild-type and mutant PBPs were measured at room temperature by the resin method as previously described (Wang et al., 1994) except that 50 mM buffer (acetate buffer at pH 4.5 or Tris−acetate at pH 8.5) was used instead of 200 mM buffer. The average and rms deviation (in parentheses) of each K_d is the result of at least three separate binding assays. Phosphate-binding affinity decreases with increasing ionic strength (Wang et al., 1994); therefore, a lower buffer concentration was used to minimize this effect. Under these conditions, the conductivity of the assay at pH 4.5 and pH 8.5 is equivalent (approximately 0.12 mho). The two pHs were chosen to ensure the presence of nearly all monobasic phosphate at low pH and dibasic at high pH. PBP binds both forms of phosphate (Luecke & Quiocho, 1990; Wang et al., 1994).

conventional positional and *B*-factor refinement. After each round, the ($2F_o - F_c$) map contoured at 1σ and the ($F_o - F_c$) map at 3σ were examined to improve, when necessary, the fit of the protein model to density and to add or delete water molecules modeled as oxygen. This examination, after the initial rounds of refinement had converged, clearly confirmed each of the mutations at residue 137 and easily allowed remodeling at the mutation site before final refinements were carried out to convergence. Only water molecules with a *B*-factor of less than 60 Å^2 were kept in the coordinate files. The statistics for the refinements are shown in Table 1. The lower *B*-factor of the 137T(Cl) structure (Table 1) reflects the lower temperature (about −130 °C) used in the data collection as compared to 4 °C for the other structures. The *R*-factors in the highest resolution shell of the data sets in Table 1, with completeness ranging from 66% to 92%, vary from 0.22 to 0.27. Structure coordinates have been deposited in the Protein Data Bank.

RESULTS AND DISCUSSION

Mutagenesis and Phosphate-Binding Activity. It was anticipated that removal of the negative charge at position 137 would eliminate a possible repulsive element in the immediate vicinity of the phosphate, at the same time significantly increasing the ionic attraction for phosphate and thereby enhancing binding affinity. As indicated in Table 2, however, eliminating the charge by replacing Asp 137 with Gly (PBP D137G), Asn (PBP D137N), or Thr (PBP D137T) had no dramatic effect on phosphate binding. For all of the proteins, binding was about 10 times tighter at pH 8.5 than it was at pH 4.5. At both pHs the affinity of PBP D137N for phosphate was virtually unchanged from wild type. The binding activity of PBP D137G is slightly enhanced (less than 2-fold), and PBP D137T is slightly reduced (about 2−3-fold) relative to wild type.

High-Resolution Structure Analysis. In search of an atomic-level explanation for the insensitivity of phosphate binding to the elimination of the Arg 135−Asp 137 salt link, the crystal structures of the mutant proteins complexed with phosphate were determined at high resolutions. The final statistics of the refinements of the wild-type and mutant PBP structures are shown in Table 1. The exceptional overall quality of the electron density maps or all the structures reflects the generally low averaged *B*-factors for the protein models (Table 1). As with the wild-type structure, the four mutant structures are very well determined, as judged by the quantitative parameters used to evaluate the correctness of the final model (Table 1; see also Materials and Methods), and, moreover, clearly confirmed the site-directed amino acid replacements (Figure 2). All the mutant structures are extremely similar to the native structure; the root-mean-square deviation of pairwise superimpositioning of α-carbons between the wild-type and mutant structures is about 0.2 Å.

Isosteric Asn to Asp Mutation Structure. To directly assess the effects of removing the negative charge at position 137, an isosteric Asn was substituted for Asp. The PBP D137N mutant structure (Figure 2a) indicates similarity of conformation between the Asn replacement and Asp of the wild type (Figure 3). Because of the high resolution of the data and excellent quality of the electron density map especially in and around the binding site cleft, the amide side chain of Asn 137 was oriented in the electron density with relative ease; Oδ1 and Nδ2 were fitted to the positions of higher density and lower density, respectively (Figure 2a). Many Asn side chains in the five refined structures exhibit a similar pattern. In a similar omit map for the wild-type PBP, the density corresponding to Asp 137 Oδ1 and Oδ2 is nearly equal. The Nδ2 of the substituted Asn is within good hydrogen bond donating distance (2.9 Å) to a water molecule (Wat 482; see also Figure 1) and also within 4.2−4.3 Å to two backbone carbonyl oxygens. Moreover, the fit of the Asn Oδ1 matches that of Asp 137 of the wild type which accepts two hydrogen bonds, one from a backbone NH group (see Figure 1).

Chloride Ion Binding in Place of Asp Carboxylate in the Mutation to Gly or Thr. As expected, in the structure of PBP D137G, a large cavity was created by the absence of the Asp 137 side chain. However, ($2F_o - F_c$) and ($F_o - F_c$) maps calculated in the initial rounds of refinement revealed a large spherical electron density within the cavity. This density was initially assumed to be a water molecule; however, because the density displayed about twice the peak height of the neighboring backbone carbonyl and side-chain oxygens, this assumption was deemed incorrect. Considering the abundant Cl^- in the solutions for growing bacterial cells, protein purification, and crystallization (Wang et al., 1995), the spherical density is more likely due to a bound Cl^- rather than a water molecule. This interpretation was corroborated by the finding that a water molecule oxygen fitted to the density refined to an inconsistent *B*-factor of 2.0 Å^2, the lowest allowed in the X-PLOR refinement. With Cl^- substituted for the water oxygen, refinement gave a reasonable halide ion *B*-factor of 16.2 Å^2 (Figure 2b). To further verify the presence of Cl^- in the 137 Gly mutant protein, the PBP D137G(Cl) crystal was soaked for 24 h in a stabilizing solution containing 50 mM KBr in place of KCl, and diffraction data were collected (see Materials and Methods and Table 1). A difference Fourier map was then calculated using ($F_{o,Br} - F_{o,Cl}$) coefficients and $\alpha_{c,Cl}$ phases. This map revealed only one difference density coincident with the Cl^- difference density (Figure 2b), which is indicative of the 18 electron difference between bromide and chloride. The PBP D137G(Br) structure was also refined (Table 1).

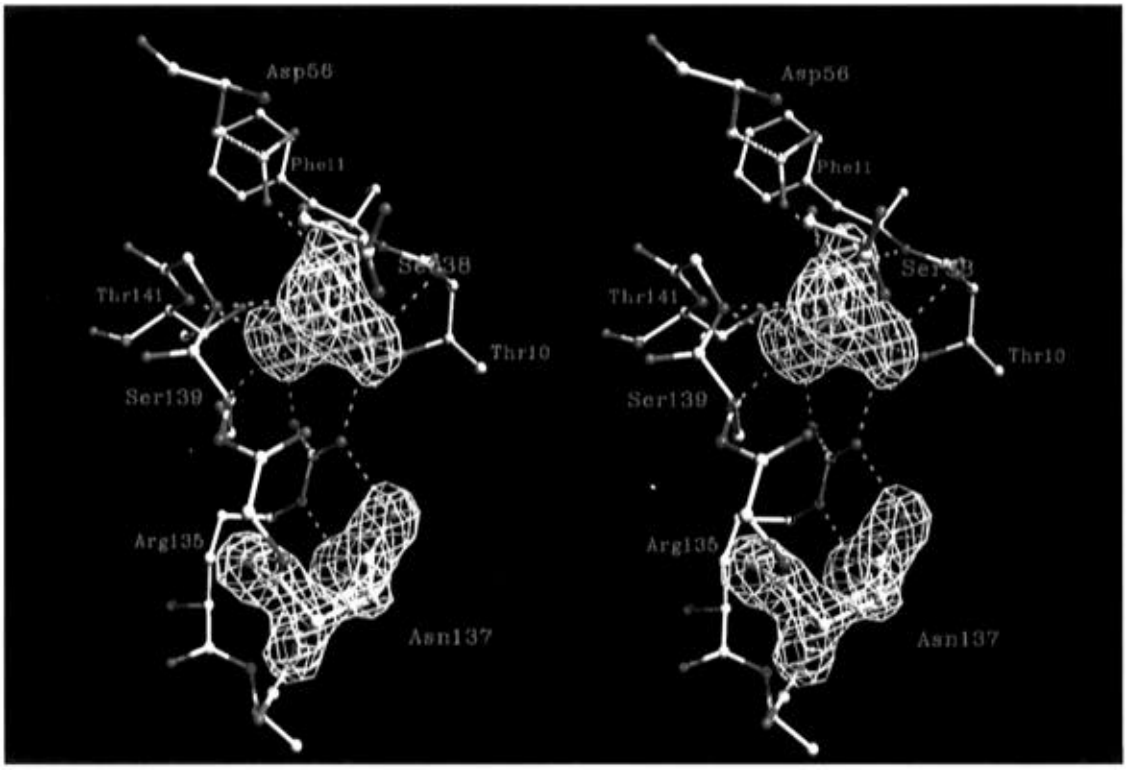
Asp56
Phe11
Thr141
Thr10
Ser139
Arg135
Asn137
Asp56
Phe11
Thr141
Thr10
Ser139
Arg135
Asn137

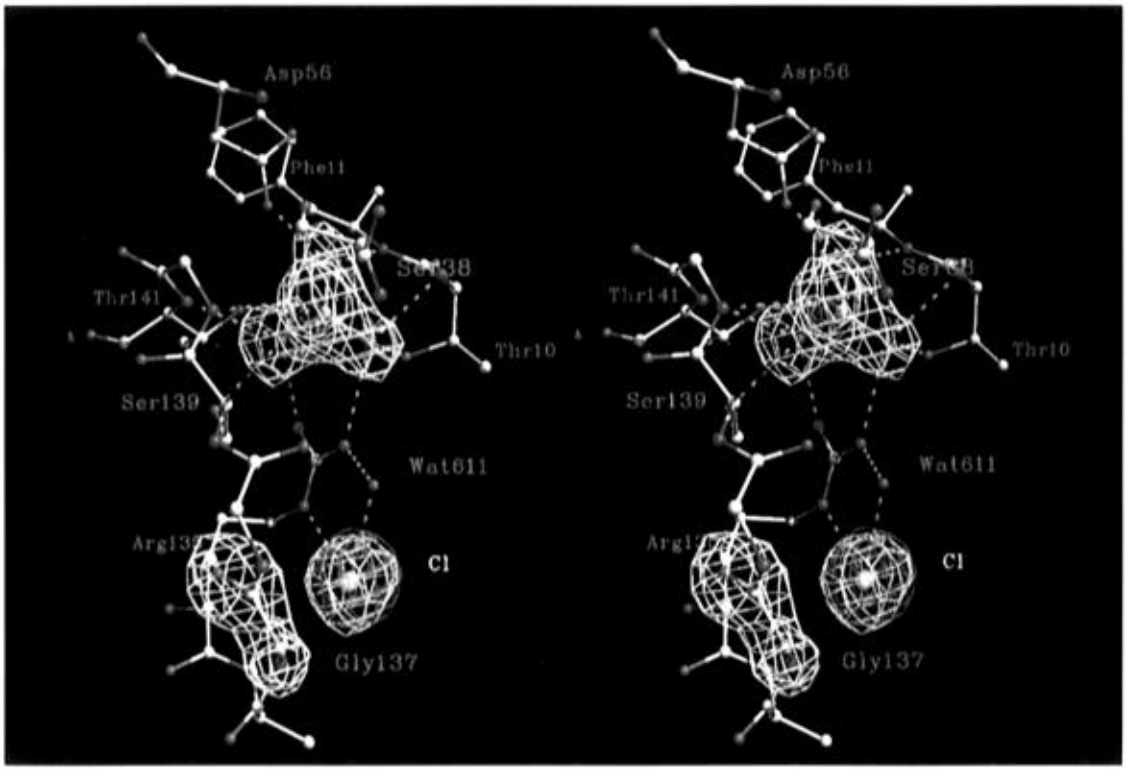
Asp56
Phe11
Thr141
Thr10
Ser139
Wat611
Cl
Gly137
Asp56
Phe11
Thr141
Thr10
Ser139
Wat611
Cl
Gly137

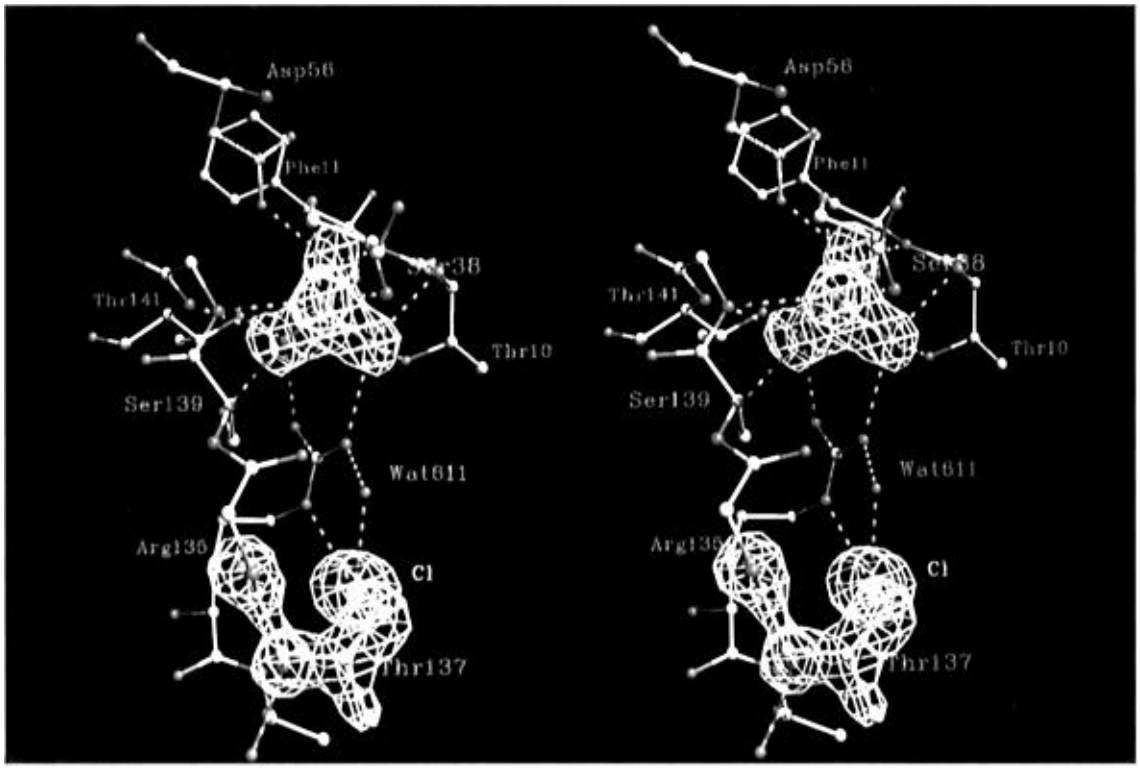

FIGURE 2: Stereoviews of the structure (ball and stick) and difference Fouriers of the sites of phosphate binding and residue 137 mutations. Atoms color codes: P, orange; O, red; N; blue, C, gray; and Cl^-, yellow. Magenta dashed lines represent hydrogen bonds or chloride coordinations. Difference density for the Asn, Gly, or Thr mutant structure, along with the bound phosphate, is contoured at 4σ and, unless specified, is represented by yellow color. Other than those shown, no significant difference density is observed in the entire asymmetric unit. (*a*, top, left page) PBP D137N mutant structure. ($F_o - F_c$) density was calculated with the contribution of Asn 137 and phosphate atoms omitted. The density peak of Asn 137 Oδ1 is about 1.7 times greater than that of Nδ2. (*b*, bottom, left page) PBP D137G(Cl) mutant structure. Difference electron density ($F_o - F_c$) was obtained by using the refined mutant structure and omitting the contributions of Gly 137, phosphate, and Cl^- in the structure factor calculation using the refined mutant structure. The red difference density was calculated using ($F_{o,Br} - F_{o,Cl}$) coefficients and $\alpha_{c,Cl}$ phases. $F_{o,Br}$ and $F_{o,Cl}$ are from the Br^- and Cl^- soaked crystals, respectively, and $\alpha_{c,Cl}$ is from the refined 1.9 Å structure of PBP D137G(Cl) (Table 1). (*c*, above) PBP D137T(Cl) mutant structure. Difference electron density ($F_o - F_c$) was obtained by using the refined mutant structure and omitting the contributions of Thr 137, phosphate, and Cl^- in the structure factor calculation.

The structures of the PBP D137G (Cl or Br) also revealed a highly localized movement of a three-residue (136−138) segment in a direction slightly away from Arg 135 relative to wild type (Figure 3). The movement is likely in response to binding of the halide ion without steric clashes. In spite of the segment movement, the ϕ and ψ values of the loop in the mutant structures remained in the allowable region.

Finally, the PBP D137T mutation was made on the assumption that the Thr side chain would occupy the area near that of the wild-type Asp or mutant Asn. However, this assumption was not validated by the structure determination (Table 1) which revealed that this Thr mutant, in a manner very similar to that of the D137G protein, also exhibited Cl^- binding and segment movement (Figures 2c and 3). These completely unpredicted results for both the Thr and Gly mutants underscore the indispensability of X-ray structures in using site-directed mutagenesis to probe protein structure and function. It is noteworthy that the presence of the highly electronegative chloride anion has very little, but opposite, effects on phosphate binding to both Gly and Thr mutant proteins (Table 2).

Invariant Receptor−Phosphate Hydrogen-Bonding Interactions. The finding that the hydrogen-bonding interactions between PBP and phosphate (Figures 2 and 3 and Table 3) are invariant in the wild-type and mutant structures indicates that the mutations had not affected the integrity of the ligand-binding site. The accuracy of the hydrogen bonds (Table 3) is consistent with the unusually well determined positions of the atoms of the phosphate and hydrogen-bonding residues. The coordinate errors estimated by Luzzati plots (not shown) predict a mean coordinate error of about 0.15 Å for all five structures listed in Table 1. However, as the region containing the phosphate and surrounding residues has about 2 times lower averaged *B*-factors than those of the protein models, the atoms in this region have coordinate deviations smaller than the mean error or more reflective of the root-mean-square deviations shown in Table 3.

Ion Binding and Charge Stabilization. The initial objective of this study was to remove an element which may be repulsive to anion binding and at the same time strengthen the ionic attraction between the protein and the phosphate by eliminating the negatively charged Asp 137. Only in the case of the Asn substitution did the mutagenesis actually serve to remove this negative charge. The incorporated Cl^- in the Gly and Thr mutant proteins takes the place of the negative charge on the wild-type Asp residue and maintains the ionic interaction with Arg 135 (Figures 2b,c and 3), thereby preventing the charge of Arg 135 from forming a salt link solely with the phosphate. Since the chloride ion is highly electronegative or a weaker Lewis base than the Asp 137 carboxylate, it has also the potential to modulate the phosphate−Arg 135 salt link. However, neither the

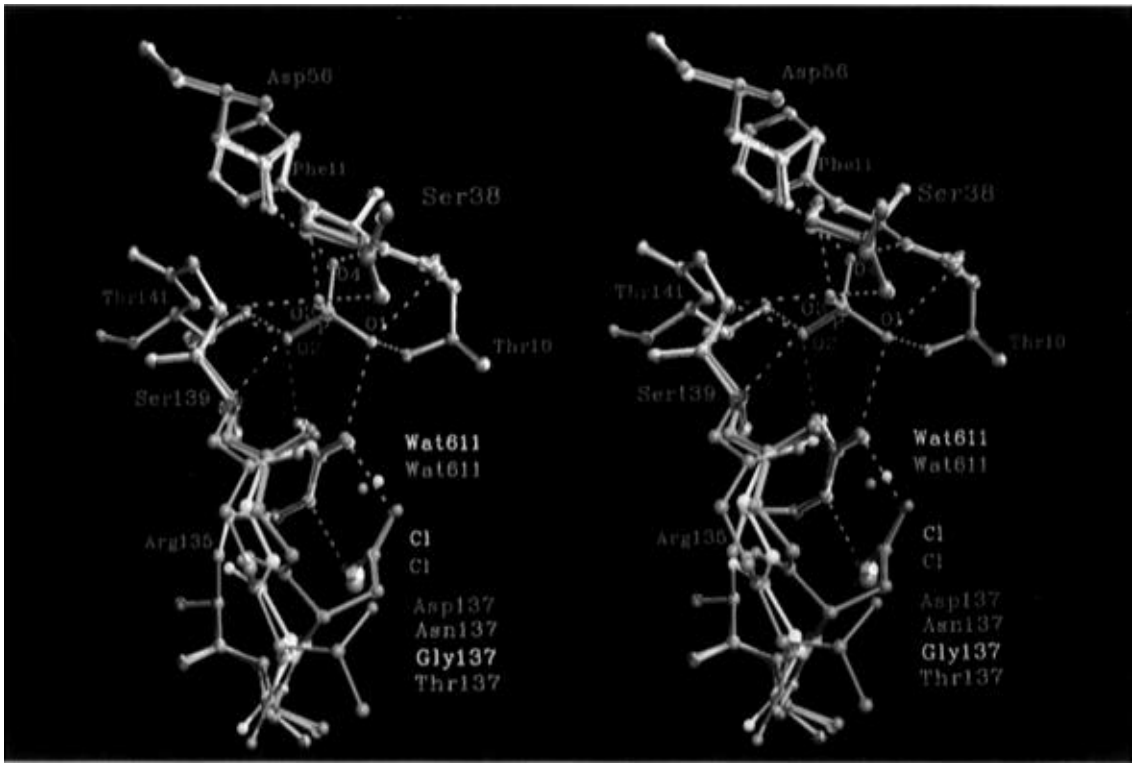

FIGURE 3: Superimposed PBP structures of the wild type (green) and mutants D137G(Cl) (yellow), D137N (orange), and D137T(Cl) (cyan). Only the contiguous area of mutation and phosphate binding is shown in identical orientation as in Figure 2. The Cl^- present in the Gly or Thr mutant structure binds in a position nearly coincident with that of the Oδ1 of Asp 137 in the native structure, making an ionic interaction with the Nϵ of the guanidinium of Arg 135 (see also Figure 2b,c). A water molecule (Wat 611), which is not present in the native structure, is in a position near the Asp Oδ2, forming a bridge between the halide ion and Nη2 of Arg 135. The bound chloride makes additional contacts (not shown) of $\leq$4 Å distance with Arg 135 Nη1, Ala 136 N, 137 Gly N, Gly 174 O, Gly176 N, and Wat 482. The Thr 137 hydroxyl group is also coordinated to the Cl^-. The largest changes, relative to the wild-type structure, in the segment of residues 136−138 are 1.6 and 1.3 Å between α-carbons of residue 137 in the mutant T137 and G137 structures, respectively.

Table 3: Hydrogen Bonds between PBP and Phosphate[a]

atom			atom		
phosphate	residue	mean distance (Å)	phosphate	residue	mean distance (Å)
O1	T10 N	2.86 (0.05)	O2	T141 Oγ1	2.73 (0.03)
O1	T10 Oγ1	2.71 (0.07)	O3	S38 N	2.80 (0.03)
O1	R135 Nη2	2.83 (0.04)	O3	S38 Oγ	2.71 (0.04)
O2	R135 Nη1	2.88 (0.02)	O3	G140 N	2.74 (0.03)
O2	S139 Oγ	2.75 (0.04)	O4	F11 N	2.88 (0.08)
O2	T141 N	2.86 (0.02)	O4	D56 Oδ2	2.43 (0.09)

[a] The mean of each hydrogen bond distance with rms deviation (in parentheses) was obtained from the five distances in the wild-type, 137N, 137G(Cl), 137G(Br), and 137T(Cl) structures.

elimination of the negative charge in the Asn mutation nor the substitution by Cl^- had any effect on the phosphate-binding activity.

In view of the presence of many local induced dipoles (including the hydrogen-bonding groups) surrounding the phosphate (Figure 1 and Table 3), the results presented do not appear unreasonable. These results indicate that, because the charge on the phosphate can be stabilized by these dipoles, binding is not dependent on, or even sensitive to, the degree of neutralization occurring by way of ionic interactions. Changes in the electric field at the phosphate caused by eliminating the negative charge or inclusion of a highly electronegative chloride ion at position 137 are presumably compensated by these dipoles, and the overall result is a near constant affinity for phosphate.

The dominant role of electrostatic interactions, especially hydrogen bonds and van der Waals interactions, in binding a charged ligand to a transport receptor is not without precedence. The complex between the sulfate-binding protein (SBP) and sulfate, which has a structure very similar to that of the PBP−phosphate complex, is notable for the absence of a salt link (Pflugrath & Quiocho, 1985). In keeping with the stringent specificity of SBP for fully ionized tetrahedral oxydianions (Pardee, 1966; Jacobson & Quiocho, 1988), the completely buried and desolvated sulfate is the recipient of seven hydrogen bonds from uncharged protein groups (Pflugrath & Quiocho, 1988). Interestingly, the lack of a salt link and fewer hydrogen bonds does not make the affinity of the SBP−sulfate complex any weaker than that of the PBP−phosphate complex. In fact, sulfate binds 10−20 times more tightly to SBP (Pardee, 1966; Jacobson & Quiocho, 1988) than phosphate does to PBP (Table 2).

Other examples of similar dipolar interaction have been pointed out (Quiocho et al., 1987), notably that of the phosphoryl group of FMN with flavodoxin which has a structure (Smith et al., 1977) similar to either of the two

domains of the periplasmic binding proteins (Gilliland & Quiocho, 1981). The essentially buried FMN phosphoryl group accepts ten hydrogen bonds, five from peptide backbone NH groups and five hydroxyl side chains (Smith et al., 1977). Similar interaction but less extensive interaction is also often observed for at least one phosphoryl group of DNA, ATP, or NAD(P) bound to proteins and enzymes. The major role of dipolar hydrogen-bonding groups and local dipoles has been implicated to be important in charge stabilization and in active transport or fast ion movement and other biochemical processes (Quiocho et al., 1987, and references cited therein; Luecke & Quiocho, 1990; Lodi & Knowles, 1993). Many of these dipolar hydrogen-bonding groups are inducible peptide backbone NH groups whose major contribution to charge stabilization has been previously investigated computationally and experimentally in these and other systems (Åqvist et al., 1991; He & Quiocho, 1993).

Although proteins and enzymes that interact with charged ligands or side chains solely through many dipolar hydrogen-bonding groups have been observed, in cases where a salt link is additionally present, it is commonly assumed that the charge interaction makes a significant contribution to complex formation. We have experimentally tested this assumption and, in the case of PBP, proven phosphate binding to be relatively insensitive to modulations of the charge. This new finding bears important ramifications in the area of ligand design and electrostatic interaction.

ACKNOWLEDGMENT

N.Y. is a Predoctoral Fellow of the W. M. Keck Computational Biology Program, a joint program of the Baylor College of Medicine, Rice University, and University of Houston. We thank Bill Meador for assistance in the diffraction data collection.

REFERENCES

Åqvist, J., Luecke, J., Quiocho, F. A., & Warshel, A. (1991) Dipoles localized at helix termini of proteins stabilize charges, *Proc. Natl. Acad. Sci. U.S.A. 88*, 2026−2030.

Brünger, A. T. (1992) *X-PLOR, Version 3.1, A system for X-ray crystallography and NMR*, Yale University, New Haven, CT.

Engh, R. A., & Huber, R. (1991) Accurate bond and angle parameters for X-ray protein structure refinement, *Acta Crystallogr., Sect. A 47*, 392−400.

Gilliland, G. L., & Quiocho, F. A. (1981) Structure of the L-arabinose-binding protein from *Escherichia coli* at 2.4 Å resolution, *J. Mol. Biol. 146*, 341−362.

He, J. J., & Quiocho, F. A. (1993) Dominant role of local dipoles in stabilizing uncompensated charges on a sulfate sequestered in a periplasmic active transport protein, *Protein Sci. 2*, 1643−1647.

Jacobson, B. L., & Quiocho, F. A. (1988) Sulfate-binding protein dislikes protonated oxyacids. A molecular explanation, *J. Mol. Biol. 204*, 783−787.

Kunkel, T. A., Roberts, J. D., & Zakour, R. A. (1987) Rapid and efficient site-specific mutagenesis without phenotypic selection, *Methods Enzymol. 154*, 367−382.

Lodi, P. J., & Knowles, J. R. (1993) Direct evidence for the exploitation of an α-helix in the catalytic mechanism of triosephosphate isomerase, *Biochemistry 32*, 4338−4343.

Luecke, H., & Quiocho, F. A. (1990) High specificity of a phosphate transport protein determined by hydrogen bonds, *Nature 347*, 402−406.

Medveczky, N., & Rosenberg, H. (1971) Phosphate transport in *Escherichia coli*, *Biochim. Biophys. Acta 241*, 494−506.

Pardee, A. B. (1966) Purification and properties of a sulfate-binding protein from *Salmonella typhimurium*, *J. Biol. Chem. 241*, 5886−5892.

Pardee, A. B., Prestidge, L. S., Whipple, M. B., & Dreyfuss, J. A. (1966) A binding site for sulfate and its relation to sulfate transport into *Salmonella typhimurium*, *J. Biol. Chem. 241*, 3962−3969.

Pflugrath, J. W., & Quiocho, F. A. (1988) Sulphate sequestered in the sulphate-binding protein of *Salmonella typhimurium* is bound solely by hydrogen bonds, *Nature 314*, 257−260.

Quiocho, F. A., Sack, J. S., & Vyas, N. K. (1987) Stabilization of charges on isolated ionic groups sequestered in proteins by polarized peptide units, *Nature 329*, 561−564.

Sack, J. S. (1988) CHAIN−a crystallographic modeling program, *J. Mol. Graphics 6*, 224−225.

Smith, W. W., Burnett, R. M., Darling, G. D., & Ludwig, M. L. (1977) Structure of the semiquinone form of flavodoxin from *Clostridum MP*. Extension of 1.8 Å resolution and some comparisons with the oxidized state, *J. Mol. Biol. 117*, 196−225.

Tam, R., & Saier, M. H. (1993) Structural, functional, and evolutionary relationships among extracellular solute-binding receptors of bacteria, *Microbiol. Rev. 57*, 320−346.

Wang, Z., Choudhary, A., Ledvina, P. S., & Quiocho, F. A. (1994) Fine tuning the specifity of the periplasmic phosphate transport receptor, *J. Biol. Chem. 269*, 25091−25094.

BI952686R